JOURNAL OF NANO- AND ELECTRONIC PHYSICS
Vol. **18** No 2, 02025(7pp) (2026)

ЖУРНАЛ НАНО- ТА ЕЛЕКТРОННОЇ ФІЗИКИ
Том **18** № 2, 02025(7cc) (2026)

OPEN ACCESS

REGULAR ARTICLE

Electrical Conductivity of Thin Films of CoNi and FeNi Alloys

V.B. Loboda*, S.M. Khursenko, V.O. Kravchenko, O.Yu. Yurchenko

Sumy National Agrarian University, 40021 Sumy, Ukraine

(Received 03 December 2025; revised manuscript received 23 April 2026; published online 29 April 2026)

This paper presents the results of the study of the electrical conductivity of structurally continuous thin films of CoNi and FeNi alloys in a wide range of thicknesses and concentrations of components. Alloy films with a thickness of 10-200 nm were obtained by condensation of evaporated initial massive binary alloys of CoNi and FeNi in a vacuum of 10^{-4} Pa. CoNi alloys were evaporated by electron beam method using an electron diode gun with a condensation rate of 0.5-1.5 nm/s. The purity of the initial metals Co and Ni was not less than 99.9%. The concentrations of components of CoNi alloy films varied in a wide range. FeNi alloy films were obtained as a result of evaporation with a 50N permafrost. Thermostabilizing of the electrophysical properties of alloy films was carried out during three heating-cooling cycles in the temperature range of 300-700 K. The dependences of the specific electrical resistance on the temperature of alloy films for the second and subsequent heating-cooling cycles practically coincide, which indicates complete stabilization of the properties of film samples after the second annealing cycle. An irreversible decrease in electrical resistance after heat treatment was experimentally revealed, which indicates ordering of the material structure. It was shown that the nature of changes in electrical resistance depends on both the thickness of the films and the ratio of components in the alloys. To interpret the obtained results, the Wend model of healing of defects in the crystalline structure of films was used, which allows us to explain the decrease in electrical resistance due to a decrease in the concentration of defects and an improvement in structural ordering. Based on this model, the spectra of defects in the crystalline structure in CoNi and FeNi alloy films were calculated.

Keywords: Nanocrystalline films, Alloys, Electrical conductivity, Crystal structure defects, Activation energy for defect healing.

DOI: 10.21272/jnep.18(2).02025 PACS numbers: 61.82.Rx, 73.61. – r

1. INTRODUCTION

Thin metal films, multicomponent film alloys and multilayer film structures are the subject of intensive research in modern condensed matter physics and nanoelectronics [1-4]. Of particular interest are films of alloys based on transition ferromagnetic metals, in particular CoNi and FeNi alloys, which combine specific magnetic and electrophysical characteristics and are widely used in sensor systems, magnetoresistive structures and spintronics elements.

The electrical conductivity of thin films significantly depends on their thickness, composition, surface morphology and structural state [5-7]. Compared with bulk materials, in films, electron scattering at crystallite boundaries, structural defects and film surfaces plays a significant role, which leads to a change in electrical resistance. This is especially evident in nanostructured films.

The processes of thermal stabilization of the electrophysical properties of thin films attract special attention. It is known that during heat treatment, relaxation processes are possible, associated with the reorganization of the crystal structure, a decrease in the concentration of defects and the enlargement of crystallites, which, as a rule, is accompanied by a change in electrical resistance. However, the mechanisms of such changes, in particular their irreversible nature, require more detailed study and theoretical justification.

In this regard, it is relevant to study the electrical conductivity of thin films of CoNi and FeNi alloys in a wide range of thicknesses and concentrations of components, as well as to establish the patterns of changes in their electrophysical properties during heat treatment. Of particular interest is the use of models that take into account the evolution of the defect structure, in particular the Wend model of defect healing, to explain the experimentally observed effects [8].

The aim of this work is to study the patterns of changes in the electrical conductivity of thin films of CoNi and FeNi alloys depending on their thickness, composition and heat treatment conditions, as well as to interpret the results obtained within the framework of the Wend model.

2. EXPERIMENTAL METHODOLOGY AND TECHNIQUE

2.1 Methodology for Studying the Electrical Conductivity of Thin Alloy Films

To study the electrical conductivity, film samples were condensed onto a polished glass plate (Fig. 1) with contact pads pre-applied at 600 K. The method and technique for producing CoNi and FeNi alloy films are

* Correspondence e-mail: loboda-v@i.ua

Cite this article as: V.B. Loboda et al., *J. Nano- Electron. Phys.* 18 No 2, 02025 (2026) https://doi.org/10.21272/jnep.18(2).02025

presented in detail in [9].

The glass plate (1) was secured to a copper substrate holder and maintained good thermal contact with it. To ensure good adhesion of the contact pad to the glass surface, the first layer was Cr with a thickness of $d \approx 50$ nm, followed by a second layer of Cu with a thickness of 150-200 nm, ensuring high electrical conductivity.

The geometric dimensions of the rectangular film were set by holes in a special mask made of nichrome foil, made with high precision (width $a = 2 \pm 0.05$ mm, length $b = 9 \pm 0.05$ mm). The mask was fixed on a substrate holder and tightly adhered to the surface of a glass plate – the substrate. This ensured the production of film samples of the same size. A dielectric film (SiO_2) was previously applied to the surface of the mask, which adhered to the substrate. This prevented shorting of contacts by the mask and allowed the electrical resistance of the films to be measured directly during the deposition process.

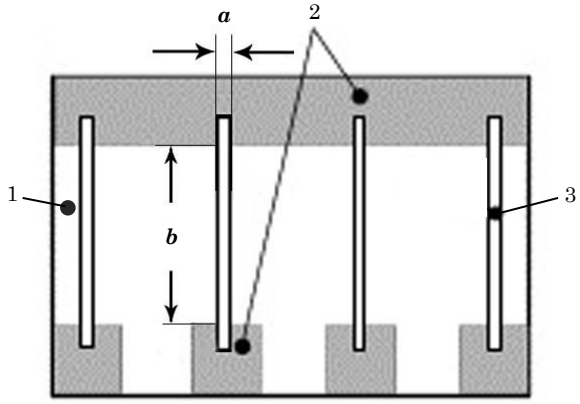

Fig. 1 – Schematic diagram of the substrate with film samples for measuring electrical resistance: 1 – glass plate; 2 – contact pads; 3 – film sample ($a = 2 \pm 0.05$ mm, $b = 9 \pm 0.05$ mm)

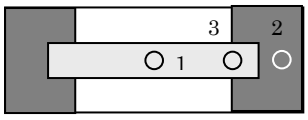

a

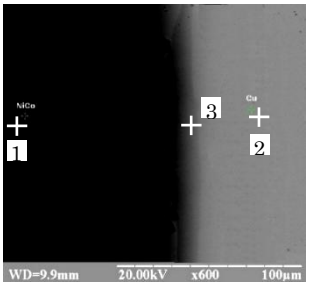

b

Fig. 2 – Scheme of film placement on a substrate with contact pads (a) and the corresponding electron microscopic image of the film surface (b): 1 – film, 2 – contact pad, 3 – film on the contact pad

The thickness of the contacts was significantly greater than the thickness of the samples, which, in combination with the low resistivity of their material (Cu), reduced the influence of the contacts on the resistance measurements. Fig. 2 shows a diagram of the film placement on the substrate and a micrograph obtained using a scanning electron microscope REM-103-01, which shows the place of application of the CoNi film to the contact pad. The figure shows that the contact area is quite uniform and when the film under study is applied to the copper contact, a defect-free (in mechanical terms) transition region is formed.

Fig. 3 shows characteristic X-ray spectra obtained using the REM-103-01 X-ray microanalyzer from the local areas marked in Fig. 2 with dimensions of 10×10 µm (for details, see [10]), by which their elemental composition was determined.

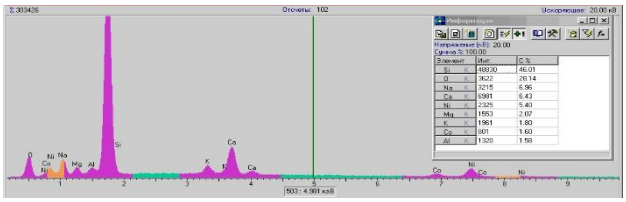

a

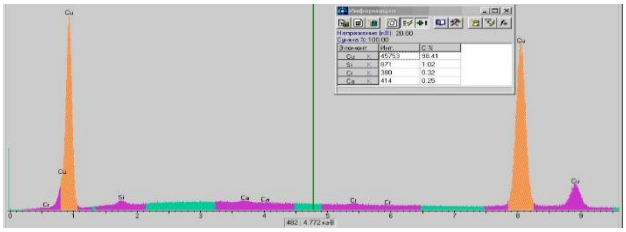

b

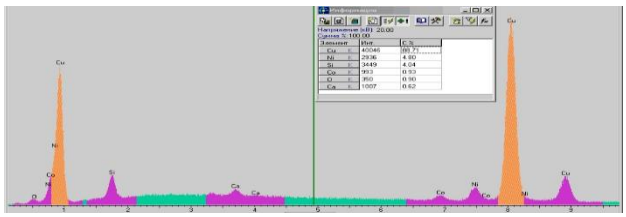

c

Fig. 3 – Characteristic X-ray spectra from the regions: a – CoNi film on a glass substrate (1 in Fig. 2); b – copper contact pad (2 in Fig. 2); c – CoNi film on a copper contact pad (3 in Fig. 2)

Analysis of the X-ray spectra shows that in the area of the CoNi film on the glass substrate (Fig. 3 a) there are only lines of the substrate material (glass) (left part of the spectrum) and the film material (right part of the spectrum). The depth of X-ray generation when probing the sample with an electron beam with an energy of 20 keV is of the order of several µm [11], which is much larger than the thickness of the studied films and contact pads. In the area of the copper pad (Fig. 3 b) there are copper lines, and in the area of the film and contact pad overlap (Fig. 3 c) there are lines of both the film material and the contact pad and the substrate. No other impurities are observed according to the micro-X-ray spectral analysis.

The resistance of the samples during the condensation process and during thermal stabilization annealing was determined using a digital voltmeter V7-34A with an accuracy of 0.01 Ohm (for films with a

resistance of more than 100 Ohm – 0.1 Ohm).

After obtaining, the film samples were kept at the substrate temperature for 30 min. Further thermal stabilization of the samples was carried out by annealing according to the scheme «heating – holding at maximum temperature – cooling» for three cycles in the range of 300-700 K in a vacuum unit VUP-5M at P = 10^{-5}-10^{-4} Pa. The substrate with the samples was fixed on a massive copper plate and had good thermal contact with it. Quartz-halogen lamps were used as heating elements of the substrate, which reduced gas evolution during heat treatment. The heating rate was 3-5 K/min. The temperature during the annealing process was controlled by a differential chromel-alumel thermocouple (the temperature measurement error did not exceed 5 K). Heat treatment for three cycles allowed obtaining films with stable properties, in particular, the temperature dependence of the electrical resistance was reproduced in the second, third and subsequent cycles with high accuracy for both CoNi and FeNi alloy films.

The film resistivity was calculated from the known geometric dimensions of the samples (width a, length b, thickness d) and the resistance R based on the relationship: $\rho = Rdab^{-1}$. The error in calculating the resistivity was primarily determined by the error in determining the thickness d and was 5-10% for films with a thickness of more than m and 10-15% for thinner films.

The temperature coefficient of resistance (TCR) was calculated based on the $R(T)$ dependences obtained during heat treatment, based on the known ratio $\beta = \Delta R/R\Delta T$. Since the geometric dimensions of the film (in particular, thickness) are not included in the formula for determining the TCR, the accuracy of determining the TCR was higher than for the resistivity and was determined by the errors in measuring the resistance and temperature.

2.2 Methodology for Calculating the Spectrum of Crystal Structure Defects

During the first heat treatment cycle, an irreversible change in resistivity is observed for most metal films [12]. It is associated with a large number of structural defects that are the cause of the violation of the equilibrium state of the structure and should disappear during heat treatment or aging. The irreversible decrease in the resistance of films during annealing or aging, according to the work of Wend [8], is associated with the healing of these structural defects. According to Wend, all defects of the crystal structure that arise during the condensation process are divided into three groups: various vacancies, pores; interstitial atoms; combined defects from vacancies and interstitial atoms. At low annealing temperatures, defects of the third group are first of all recombined, since this does not require diffusion of atoms over significant distances. To start the recombination process, it is necessary to provide the atom with some energy E_m, the value of which lies in the range from zero to the activation energy of diffusion or self-diffusion of atoms of the film material.

If $r(E)$ is the contribution to the residual resistance due to the formation of one defect per unit volume, then the total resistivity due to the presence of defects can be written as [13]:

$$\rho = \int_{(E)} r(E)N(E,t)dE \tag{2.1}$$

where t is the annealing time required to reach the temperature T at which ρ is measured; $N(E, t)$ is the number of defects per unit volume with healing energy from E to $E + \Delta E$.

The value of $N(E, t)$ is found from the relation:

$$\frac{dN(E,t)}{dt} = -cN(E,t)\,exp\left(-\frac{E}{kT}\right) \tag{2.2}$$

where k is the Boltzmann constant.

The coefficient $c = 4\omega_{max}/2\pi$ (n is the number of atoms forming the defect, estimated to be approximately 10 [8]; $\omega_{\max} = k\Theta_D/\hbar$ is the maximum frequency of thermal vibrations of the crystal lattice atoms, associated with the Debye temperature of the film Θ_D).

The quantities $r(E)$ and $N(E, t)$ are associated with the defect distribution function, which can be represented as follows:

$$F_0(E) = -\frac{1}{kU}\frac{\partial\rho}{\partial T} \tag{2.3}$$

where $\frac{\partial\rho}{\partial T}$ is the slope of the curve of the dependence of the specific resistance on temperature when heating at a constant rate;

$$U = \frac{n(u+2)}{u+1}$$

$$E = ukT$$

The value of u is determined from the equation

$$u + lg\,u = lg\frac{4nt\omega_{max}}{2\pi} \tag{2.4}$$

To find the value $\frac{\partial\rho}{\partial T}$, a correction must be made to account for the normal change in resistance with temperature. Then

$$\frac{\partial\rho}{\partial T} = \frac{\partial\rho_1}{\partial T} - \frac{\partial\rho_2}{\partial T} \tag{2.5}$$

$\frac{\partial\rho_1}{\partial T}$ and $\frac{\partial\rho_2}{\partial T}$ are the changes in film resistivity in the first and second annealing cycles.

Having constructed the dependence $F_0(E)$, we obtain the energy spectrum of defects that cause deformations in the thin film. This dependence has the form of a curve with one or more maxima, which correspond to defects with different healing activation energies E_m. The contribution to the total resistance of those defects that have a healing energy from E_1 to E_2 can be determined by calculating the area under the curve.

$$\int_{E_1}^{E_2} F_0(E)dE \tag{2.6}$$

3. RESULTS AND DISCUSSION

As noted earlier, to stabilize the physical properties, the film samples were heat treated by heating to a temperature of 700 K. In the graphs of the dependences of electrical resistance on temperature (Fig. 4), obtained during the heating process during the first

cycle of heat treatment, three sections can be conditionally distinguished. The first of them is characterized by a slight change (most often an increase) in resistance and a value of TCR close to zero. For films with small thicknesses (d < 25-30 nm), this section is not observed (Fig. 4 a). In the second section, for all samples, regardless of their composition and thickness, a significant decrease in resistivity occurred. It is believed that a similar course of the $\rho(T)$ curve is associated with the restructuring of the non-equilibrium structure of the samples under the influence of temperature. With a sufficiently large film thickness (over 50 nm), a third section is also observed during the first annealing cycle, in which a typical metallic dependence $R(T)$ is manifested. When moving to films with a concentration of more than 60-70 wt.% Co, this area becomes less clearly pronounced, a slight decrease in resistance is observed up to the maximum temperature (Fig. 4 d). This course of the resistivity dependence can be associated with the healing of defects in the crystal structure and the passage of recrystallization processes. An increase in the size of crystallites and improvement of the structure reduces the effect of scattering of conduction electrons on defects, which is manifested in a decrease in electrical resistance.

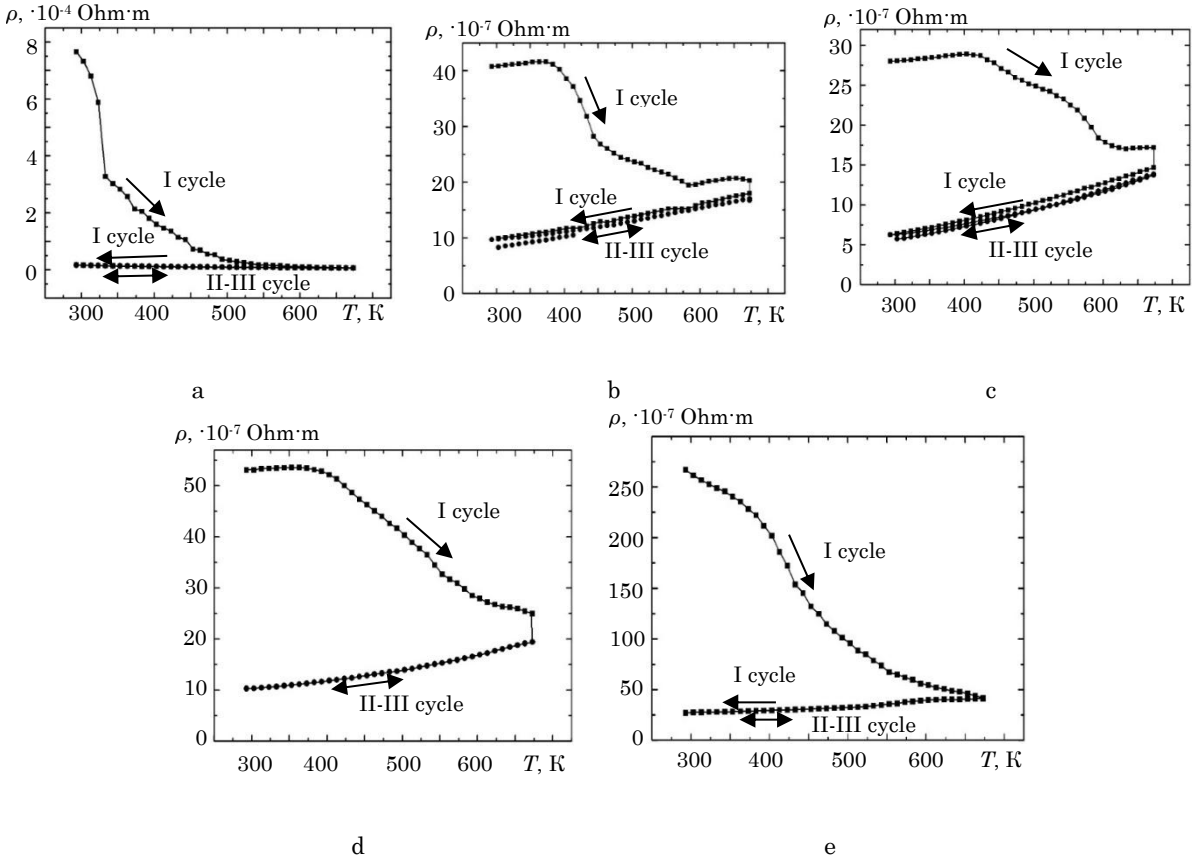

Fig. 4 – Change in the resistivity of CoNi film alloys during thermal stabilization: a – $Co_{20}Ni_{80}$, d = 18 nm; b – $Co_{20}Ni_{80}$, d = 80 nm; c – $Co_{40}Ni_{60}$, d = 54 nm; d – $Co_{90}Ni_{10}$, d = 70 nm; e – $Co_{90}Ni_{10}$, d = 44 nm

The decrease in electrical resistance in the second section (Fig. 4 b-d) for fairly thick films was 3-5 times, while in the case of small thicknesses the resistivity decreased by 10-50 times, and in some cases (for ultrathin samples with $d < 20$ nm) its decrease took place by 2-3 orders of magnitude. The relatively small decrease in resistance in the case of thicker films ($d > 50$ nm) is most likely due to the fact that partial self-healing of defects occurs already during the condensation of a thick film. For films with a thickness of more than 50 nm, the temperature at which the decrease in resistance began was 380-400 K, for thinner films it decreases (in particular, for thicknesses $d \leq 25$ nm the decrease in resistance began immediately after the start of annealing, the first section is absent). This change can be explained by the greater defect content of the structure of thin films compared to thicker ones, as a result of which the healing processes can begin at lower temperatures and have a lower activation energy E_m.

Experimental curves of changes in resistivity during the first and second thermal stabilization cycles (Fig. 4) were used by us to calculate the spectrum of defects in thin films of the CoNi alloy according to Wend. Typical dependences of $F_0(E)$ for films of approximately the same thickness (d = 60 nm) and different Co contents are given in Fig. 5 and Fig. 6. For film CoNi alloys, the presence of three types of structural defects with activation energies E_{m1} = 0.55-0.64 eV, E_{m2} = 0.73-0.75 eV and E_{m3} = 0.80-0.84 eV can be noted. For films with a Co content of more than 80 wt.% (Fig. 5 b), the appearance of another maximum is observed, which corresponds to an activation energy of 0.95-1.0 eV.

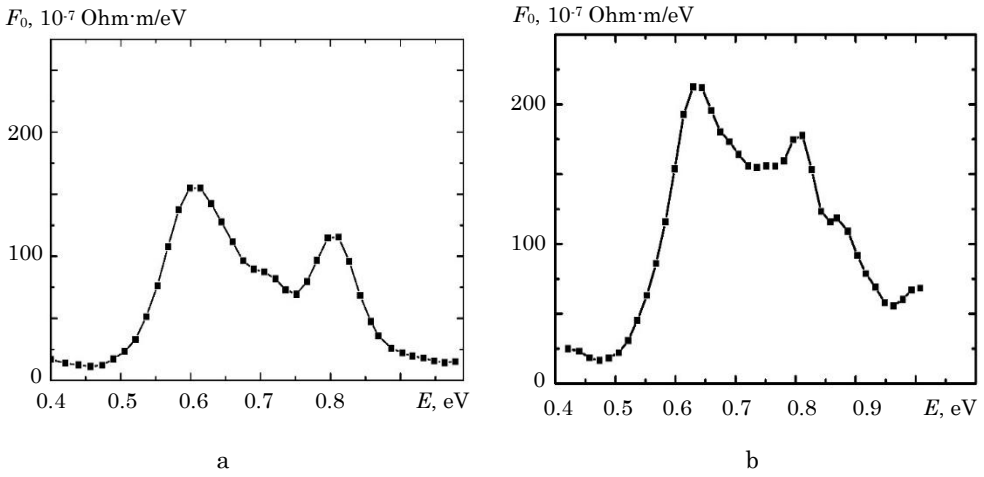

Fig. 5 – Typical dependences of the defect distribution function $F_0(E)$ for CoNi films with a thickness of $d = 60$ nm: a – $C_{Co} = 20$ wt.%, b – $C_{Co} = 90$ wt.%

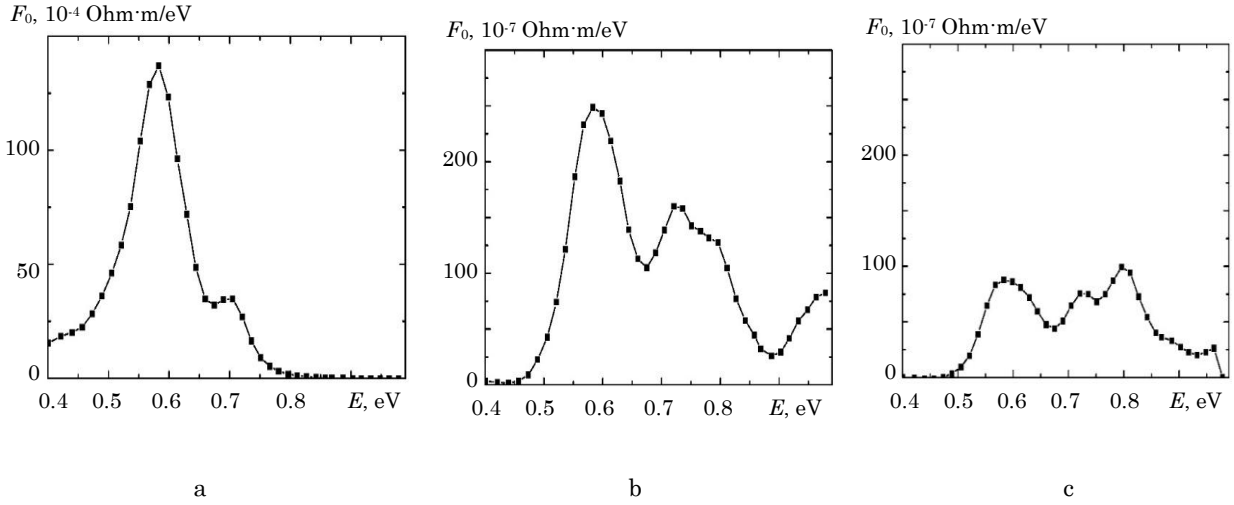

Fig. 6 – Dependences of the defect distribution function $F_0(E)$ for CoNi films with a Co content of $C_{Co} = 80$ wt%. Film thickness: a – $d = 20$ nm, b – $d = 60$ nm, c – $d = 110$ nm

Before discussing the results obtained, it should be noted that we are not aware of any work where the Wend method was applied to calculate the defect spectrum in CoNi film alloys. For NiCu film alloys [14], it was found that in the defect spectra of the crystal structure of these alloys, two maxima are observed with healing energies $E_{m1} = 0.46$-0.51 eV and $E_{m2} = 0.58$-0.64 eV for films of approximately the same thickness, which is slightly less than for the films of our alloys. Most likely, this is due to the smaller crystallite sizes in CoNi alloy films compared to CuNi alloy films and the larger values of the self-diffusion energy E_S of Co and Ni atoms ($E_S = 2.9$-2.95 eV) compared to the self-diffusion energy of Cu atoms ($E_S = 2.05$ eV) [15].

With increasing film thickness, no significant shift of the maxima was observed, but the defect spectrum undergoes changes (Fig. 6). Samples with a small thickness have a much more defective structure (Fig. 6 a), and the largest contribution is from defects with a low healing activation energy. With increasing film thickness, the ratio of contributions of defects with different energies becomes commensurate (Fig. 6 b, c) with a simultaneous decrease in the total number of defects. This result explains the reason for the absence of the first section on the $\rho(T)$ dependence for thin films for the first cycle and the rapid drop in resistance at the beginning of annealing. The appearance of several sections with different rates of resistance decrease (Fig. 4 b-d) during the first heating cycle corresponds to an increase in the fraction of defects with a higher healing activation energy. As in [14], it can be argued that one of the possible types of defects in films is the combination of «vacancy – impurity gas atom from the residual atmosphere». Most likely, the maximum with energy E_{m1} corresponds to this type of defects, and their contribution to the total resistance for very thin films is decisive due to the relatively large contribution of atoms of the near-surface layers to the total number of atoms in the film and, possibly, low condensation rates. In thicker films, the near-surface layer, enriched with impurity atoms of the residual atmosphere gas, has a smaller effect on the resistance of the films, and the contribution of other types of defects localized in the volume of the film itself increases.

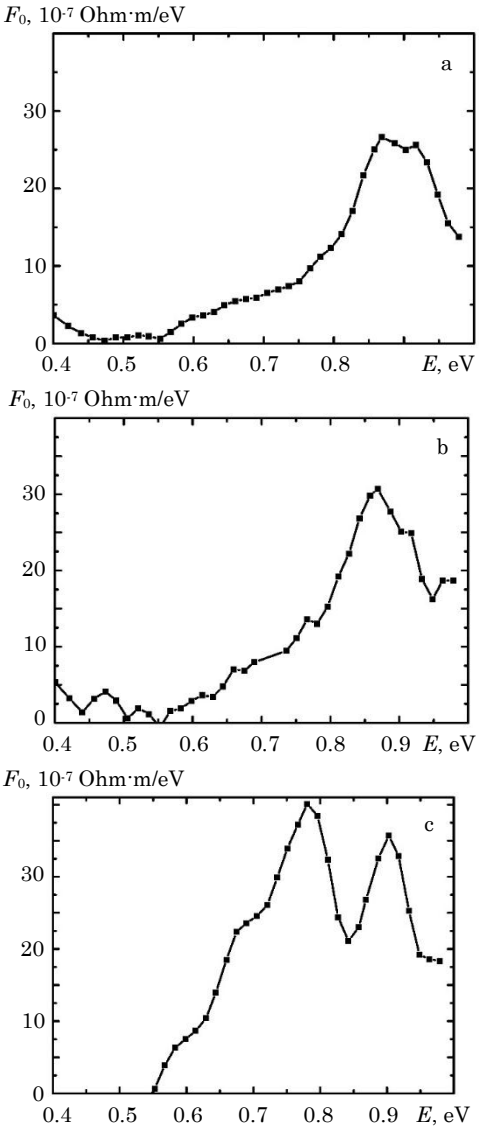

Fig. 7 – Defect spectrum of FeNi alloy films. Film thickness: a – d = 45 nm, b – d = 75 nm, c – d = 120 nm

A characteristic feature of CoNi films with a thickness of d < 20-25 nm is a sharp (Fig. 4 a) drop in resistance during the first annealing compared to thicker films (Fig. 4 b-d). This can be considered a sign of the presence of an initial amorphous structure of the films.

The third area, which is observed during the first heating and in which the resistance increases with temperature, is obviously associated with the end of the recrystallization processes and the transition in the first heat treatment cycle to the typical character of the resistance change with temperature for metals.

During the cooling process after the first cycle and in subsequent heat stabilization cycles, there are no significant changes in the resistivity, and the course of the $\rho(T)$ dependence is reproduced with high accuracy (Fig. 4 a-d).

For FeNi alloy films, the temperature dependences of the electrical conductivity during heat stabilization annealing are similar to those for CoNi alloy films. The corresponding calculations of the defect spectra indicate the presence of two maxima with energies of 0.77-0.80 eV and 0.90-0.95 eV (Fig. 7).

For FeNi alloy films, lower values of the defect distribution function $F_0(E)$ are observed even for thicknesses of 40-60 nm. The absence of maxima with low activation energy values may be due to the higher chemical activity of iron.

4. CONCLUSIONS

1. The dependence of the specific electrical resistance on the temperature ρ(T) of the films of CoNi and FeNi alloys for the second and subsequent "heating-cooling" cycles practically coincide, which indicates the complete stabilization of the properties of the film samples already after the second annealing cycle.

2. Spectra of crystal structure defects in freshly condensed films of CoNi and FeNi alloys were calculated on the basis of Wend's method.

3. The observed maxima with defect healing activation energies of less than 1 eV belong, in most cases, to the "vacancy – impurity atom from the final atmosphere" complex.

REFERENCES

1. P.H. Wu, N. Liu, W. Yang, Z.X. Zhu, Y.P. Lu, X.J. Wang, *Mater. Sci. Eng.: A* **642**, 142 (2015) https://doi.org/10.1016/j.msea.2015.06.061.
2. Yu.O. Shkurdoda, A.M. Chomous, Yu.M. Shabelnyk, L.V. Dekhtyaruk, V.B. Loboda, S.M. Khursenko, *10th International Conference on Nanomaterials Applications and Properties (NAP-2020)*, art. no. 9309616 (Sumy: Sumy State University: 2020). https://doi.org/10.1109/NAP51477.2020.9309616.
3. V.K. Soni, S. Sanyal, S.K. Sinha, *Vacuum* **174**, 109173 (2020) https://doi.org/10.1016/j.vacuum.2020.109173.
4. G. Li, G. Song, N. Wang, *Surf. Interface* **28**, 101651 (2022) https://doi.org/10.1016/j.surfin.2021.101651.
5. I. Yu. Protsenko, P.K. Mehta, L.V. Odnodvorets, C.J. Panchal, K.V. Tyshchenko, Yu.M. Shabelnyk, N.I. Shumakova, *J. Nano- Electron. Phys.* **6**, No 1, 01031 (2014).
6. L. Odnodvorets, S. Protsenko, O. Synashenko, D. Velykodnyi, I. Protsenko, *Crystal Research and Technology* **44** No 1, 74 (2009) https://doi.org/10.1002/crat.200800160.
7. A.D. Pogrebnjak, Y. Bing, M. Sahul, *Nanocomposite and Nanocrystalline Materials and Coatings. Microstructure, Properties and Applications*, 236 (Singapore: Springer: 2024). https://doi.org/10.1007/978-981-97-2667-7.
8. V. Vand, *Proceedings of the Physical Society* **55** No3, 222 (2002).
9. V.B. Loboda, S.M. Khursenko, V.O. Kravchenko, *Adv. Struct. Mater.* **214**, 201 (2024). https://doi.org/10.1007/978-981-97-2667-7_8.
10. V.B. Loboda, V.M. Zubko, S.M. Khursenko, V.O. Kravchenko, A.V. Chepizhnyi, *J. Nano-Electron. Phys.* **15** No5, 05014 (2023). https://doi.org/10.21272/jnep.15(5).05014.
11. J.I. Goldstein, D.E. Newbury, P. Echlin, D.C. Joy, C.E. Lyman, E. Lifshin, J.R. Michael. *Scanning Electron*

Microscopy and X-ray Microanalysis (New York: Springer Science + Business Media: 2003). https://doi.org/10.1007/978-1-4615-0215-9.
12. H. Frey, H.R. Khan. *Handbook of Thin-Film Technology* (Berlin: Springer-Verlag: 2015). https://doi.org/10.1007/978-3-642-05430-3.
13. I. Turek, T. Zalezak, *J. Phys.: Conf. Ser.* **200**, 052029 (2010). https://doi.org/10.1088/1742-6596/200/5/052029.
14. V.B. Loboda, S.M. Khursenko, V.O. Kravchenko, V.M. Zubko, *J. Nano-Electron. Phys.* **18** No1, 01013 (2026). https://doi.org/10.21272/jnep.18(1).01013.
15. W.F. Gale, T.C. Totemeier, *Smithells Metals Reference Book* (Heinemann: Elsevier Butterworth: 2004). ISBN: 978-0-7506-7509-3.

Електропровідність тонких плівок сплавів CoNi та FeNi

В.Б. Лобода, С.М. Хурсенко, В.О. Кравченко, О.Ю. Юрченко

Сумський національний аграрний університет, 40021 Суми, Україна

У даній роботі представлені результати дослідження електропровідності структурно суцільних тонких плівок сплавів CoNi та FeNi в широкому інтервалі товщин і концентрацій компонентів. Плівки сплавів завтовшки 10-200 нм були отримані конденсацією випарених вихідних масивних бінарних сплавів CoNi та FeNi у вакуумі 10^{-4} Па. Сплави CoNi випаровувалися електронно-променевим способом за допомогою електронної діодної гармати зі швидкістю конденсації 0,5-1,5 нм/с. Чистота вихідних металів Co та Ni становила не менше 99,9%. Концентрації компонент плівок сплаву CoNi змінювалися в широкому діапазоні. Плівки сплаву FeNi були отримані в результаті випаровування пермалою 50Н. Термостабілізація електрофізичних властивостей плівок сплавів здійснювалася протягом трьох циклів «нагрівання-охолодження» в діапазоні температур 300-700 К. Залежності питомого електроопору від температури плівок сплавів для другого і наступних циклів «нагрівання-охолодження» практично збігаються, що свідчить про повну стабілізацію властивостей плівкових зразків вже після другого циклу відпалювання. Експериментально виявлено необоротне зменшення електроопору після термічної обробки, що свідчить про упорядкування структури матеріалу. Показано, що характер змін електроопору залежить як від товщини плівок, так і від співвідношення компонентів у сплавах. Для інтерпретації отриманих результатів використано модель Венда заліковування дефектів кристалічної структури плівок, яка дозволяє пояснити зниження електроопору за рахунок зменшення концентрації дефектів і покращення структурної впорядкованості. На основі цієї моделі було розраховано спектри дефектів кристалічної структури у плівках сплавів CoNi та FeNi.

Ключові слова: Нанокристалічні плівки, Сплави, Електропровідність, Дефекти кристалічної структури, Енергія активації залікування дефектів.